Preprints of the 22nd IFAC World Congress
Yokohama, Japan, July 9-14, 2023

Online feedforward parameter learning with robustness to set-point variations

Thijs van Keulen [*,**] **Tom Oomen** [*] **Maurice Heemels** [*]

[*] *Eindhoven University of Technology, Department of Mechanical Engineering, Control Systems Technology group, (e-mail: t.a.c.v.keulen(at)tue.nl)*
[**] *ASML, Veldhoven, the Netherlands*

Abstract: High-tech motion system development is driven by increasingly accurate and fast positioning requirements. Feedforward compensation together with high bandwidth feedback control are essential to achieve these ever tightening performance demands. In particular, online adaptation of the feedforward parameters, to correct for small position dependencies and slow variations, is crucial to approach zero error tracking. The aim of this paper is a framework that provides robust recursive learning of feedforward parameters for any bounded reference trajectory. The convergence of the parameter learning strategy exploits the difference in time-scale between the parameter variation rate and the bandwidth of the servo controlled system. This enables to describe a servo-error-based objective function for varying trajectories as a static sector bounded nonlinearity. Subsequently, the circle criterion is employed to derive stability guarantees on the learning with explicit robustness to reference trajectory variation. A numerical case study demonstrates that a significant performance improvement can be achieved.

Keywords: Iterative and repetitive learning control, Extremum seeking and model free adaptive control, Continuous time system estimation

1. INTRODUCTION

High-tech motion systems, such as wafer stages in lithography machines (Butler, 2011; Heertjes et al., 2020), Atomic Force Microscopes (Kara-Mohamed et al., 2015), or industrial flatbed printers (Blanken et al., 2020), execute positioning tasks with extreme demands on throughput and accuracy. To achieve fast and accurate positioning, these systems heavily rely on FeedForward (FF) compensation alongside high bandwidth Feedback (FB) control. Typical FF compensation for position reference trajectory induced disturbance forces includes acceleration and snap FF compensation parameters, see Boerlage et al. (2004); Boerlage (2006). Moreover, careful design of the set-point trajectory is needed to balance fast movements with moderate excitation of the mechanical structure, see Lambrechts et al. (2005); Biagiotti and Melchiorri (2012).

1.1 Motivation for online feedforward parameter learning

Small variations in the system, e.g., due to slow thermal transients, leads to limited accuracy that is achievable with offline calibration of the FF parameters. Simultaneous online estimation of the sub-optimal parameters over a receding horizon of past data and immediate adaptation of the FF parameters, to correct for position dependency and slow variations, is needed to approach zero error tracking.

1.2 Overview of learning strategies

To enhance the tracking performance of high-tech motion systems beyond what can be achieved with constant FF parameters, learning strategies are explored that can improve the future control performance by evaluating the actual measured tracking performance.

Iterative Learning Control (ILC) is a learning approach (Arimoto et al., 1984) that improves the control performance of systems that perform a repeating positioning task by mapping the measured servo error along one iteration to a compensation trajectory for the next iteration, see Bristow et al. (2006) for an overview, and Rotariu et al. (2008) for application of ILC to high-tech motion systems. A known challenge for ILC is to achieve sufficient robustness of the learning to variations of the set-point (Rotariu et al., 2008; van Zundert et al., 2016). Although high-tech motion systems are designed for specific tasks, unfortunately, exact repetition of reference trajectories can often not be guaranteed in complex motion systems. Moreover, the system properties may vary within the time-scale of a typical repeating positioning task.

In van de Wijdeven and Bosgra (2010); Hoelzle et al. (2011); Bolder and Oomen (2015); van Zundert et al. (2016), the robustness of ILC to set-point variations is enhanced by the introduction of basis functions. Basis functions map the reference signal with a relatively small parameter set to the FF signal. Hence, the application of basis functions strongly reduces the dimensionality of the mapping from servo error to control input by capturing the behaviour of the system induced by the reference trajectory using a condensed output space. An example basis function is the derivative operator that provides higher-order derivatives of position, i.e., acceleration, jerk, snap, etc.

The application of basis functions is also explored in the data-driven Iterative Feedback Tuning (IFT) approach, see van de Meulen et al. (2008); Baggen et al. (2008); Cao et al. (2020), for results in the context of motion systems, and Hjalmarsson (2002) for a general overview. IFT constructs an objective function based on the inner product of a measured servo error over a selected interval. In Boeren et al. (2015), it is demonstrated that the IFT application to FF parameter tuning in van de Meulen et al. (2008); Baggen et al. (2008), is in essence a least-squares solution to a parameter identification problem, however, with a regressor that contains correlated measurement noise leading to bias. To avoid bias in the parameter estimation, the utilization of basis function is further investigated in Boeren et al. (2015, 2017) and it is shown that the application of basis functions can be viewed in the context of Instrumental Variable (IV) parameter identification, see Söderström and Stoica (1984).

To summarize, effective learning strategies are developed for systems that operate with a batch repetitive servo task in which it is well understood that the exploitation of the set-point characteristics in the form of IV enables bias-free optimal compensation parameter estimates. Nevertheless, the optimization of parameters that vary with a time-scale shorter than the batch task cannot benefit from these iterative learning approaches.

The optimal FF controller must reflect the reciprocal of the system dynamics. Therefore, adaptive control approaches provide learning of FF parameters on the basis of plant input (force) and output (position) measurements (Butler, 2012; Mooren et al., 2019). Parameter adaptation is obtained by solving this parameter estimation problem recursively in, e.g., a least-squares fashion. Unfortunately, recursive parameter adaptation based on both input and output data is sensitive to bias in the parameter estimation due to measurement noise in the output signal. In Mooren et al. (2019), the bias due to measurement noise is partly mitigated by the application of a low-pass filter. In Mooren et al. (2022), an IV approach for recursive FF estimation is developed. This leads to consistent estimates, yet requires a detailed specification of statistical properties.

The aim of the current paper is to develop a deterministic recursive learning approach. To overcome the dependency between parameter estimation and recursive parameter adaptation, a continuous-time approach is developed that exploits time-scale separation and resembles Extremum Seeking Control (ESC) Krstić and Wang (2000); Nešić et al. (2012). ESC provides optimization by online estimation of the local derivative of a constructed objective functional and to adjust the control input by, e.g., a steepest descent feedback control. Time-scale separation plays a pivotal role in the convergence analysis of ESC where the parameter updating is required to be slow compared to the derivative parameter estimation.

1.3 Contribution

The main contributions of this paper is to provide a continuous-time parameter learning framework that is robust to any bounded set-point trajectory. The second contribution is to showcase the FF parameters optimization framework in a numerical case study.

1.4 Organization

The organisation of this article is as follows. Section 2 provides a description of the control design for high-tech motion systems. Section 3 provides the main result which is a novel learning framework. A numerical case study is given in Section 4. Finally, conclusions are drawn in Section 5.

2. CONTROL DESIGN FOR HIGH-TECH MOTION SYSTEMS

This section describes a typical control design for high-tech motion systems. To achieve accurate tracking, the design includes a combination of FB and FF control and set-point Trajectory Planning (TP), see Fig. 1 for a schematic overview of the control design.

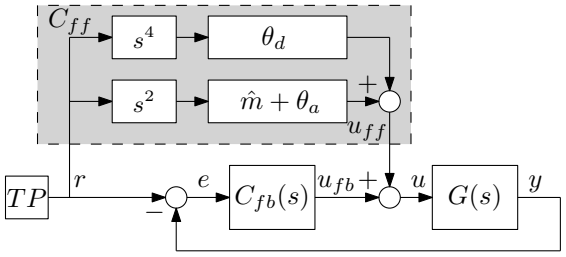

Fig. 1. Schematic overview of the controlled system $G(s)$ with feedforward C_{ff} and feedback C_{fb}.

2.1 Plant dynamics

For the design of the FB and FF control in high-tech motion systems it is convenient, see Boerlage et al. (2004); Boerlage (2006); Heertjes et al. (2017), to decompose the plant description in:

$$G(s) = \frac{1}{ms^2} + G_{flex}(s). \tag{1}$$

Here, $m \in \mathbb{R}$ is the mass, and the n flexible modes of $G_{flex} \in \mathbb{C}$ are described by the transfer function:

$$G_{flex}(s) = \sum_{i=2}^{n} \frac{\phi_i}{m\left(s^2 + 2\xi_i\omega_i s + \omega_i^2\right)}, \tag{2}$$

in which ω_i is the i-th resonance frequency, ξ_i is the modal damping of the i-th flexible mode, and $\phi_i \in [-1, 1]$ the mode gain. The compliance of the mechanical structure provides the static contribution:

$$G_{flex0} \coloneqq G_{flex}(0) \in \mathbb{R}. \tag{3}$$

2.2 Feedforward compensation of the plant dynamics

Feedforward compensation is employed to enhance the tracking performance. A common FF strategy is to compensate the reciprocal rigid-body plant behavior which is known as mass or acceleration FF by $\hat{m}s^2$. Here, $\hat{m}$ is an estimate of the plant's mass obtained by offline calibration. The difference between the offline estimate and the true (unknown) mass is described by:

$$\theta_a \coloneqq m - \hat{m}. \tag{4}$$

Assumption 1. Offline calibration of the mass parameter can provide a good estimate $\hat{m}$ such that $\left|1 - \frac{m}{\hat{m}}\right| \ll 1$.

Implementation of acceleration FF in flexible systems cannot remove the tracking error completely. Further improvement of the tracking performance is obtained by snap FF (Boerlage et al., 2004; Boerlage, 2006), which compensates for the static contribution of all flexible modes:

$$\theta_d \coloneqq -\hat{m}^2 \hat{G}_{flex0}. \tag{5}$$

The FF compensation parameters can now be collected in $\theta \in \mathbb{R}^{1\times 2}$:

$$\theta \coloneqq [\theta_a \ \theta_d]^\top, \tag{6}$$

such that the following FF controller is obtained:

$$C_{ff}(s,\theta) \coloneqq (\hat{m} + \theta_a)\, s^2 + \theta_d s^4. \tag{7}$$

This FF controller can be parameterized in terms of basis functions as follows:

$$C_{ff}(s,\theta) = \hat{m}s^2 + \sum_{i=1}^{2} \Psi_i(s)\theta_i, \tag{8}$$

in which $\theta_i \in \mathbb{R}$ is the "ith" scalar element of θ and with the basis functions:

$$\psi_1(s) = s^2, \tag{9}$$

$$\psi_2(s) = s^4. \tag{10}$$

2.3 Feedback control

Feedback control is employed to reject unknown disturbances, measurement noise, and FF model mismatch.

The FB can be represented by an idealized Proportional, Integral, Derivative (PID) controller appended with a second order low-pass filter, see, e.g., Heertjes et al. (2020):

$$C_{pid}(s) = \frac{k_d s^2 + k_p s + k_i}{s} \cdot \frac{\omega_{lp}^2}{s^2 + 2\beta_{lp}\omega_{lp}s + \omega_{lp}^2}, \tag{11}$$

where k_d, k_p and k_i are the PID FB parameters, respectively, ω_{lp} the low-pass filter cut-off frequency, and β_{lp} the filter damping ratio. To maximize disturbance rejection the aim is to achieve a high control bandwidth ω_b, i.e., where $|C_{fb}(j\omega_b)G(j\omega_b)| = 1$.

The flexible modes (2) are usually bandwidth limiting. Notch filtering can be employed to enhance the control bandwidth:

$$C_{notch}(s) = \prod_{i=1}^{q} \left(\frac{s^2 + 2\beta_{z,i}\omega_{z,i}s + \omega_{z,i}^2}{s^2 + 2\beta_{p,i}\omega_{p,i}s + \omega_{p,i}^2} \right), \tag{12}$$

in which, $\beta_{z,i}$ and $\beta_{p,i}$ are the damping parameters, and $\omega_{p,i}$ and $\omega_{z,i}$ are the notch, pole, and zero frequency of the qth notch filter, respectively. The FB controller is thus given by:

$$C_{fb}(s) = C_{pid}(s)C_{notch}(s). \tag{13}$$

The transfer function

$$e = S(s)r, \tag{14}$$

in which

$$S(s) = \frac{1}{1 + G(s)C_{fb}(s)}, \tag{15}$$

describes the sensitivity of the FB controller.

Assumption 2. A parametrization of (11) and (12) is available that for system (1) provides stable closed-loop behaviour, i.e. where all poles of (15) are located in the open left half of the complex plane.

Consider, e.g., Heertjes et al. (2020) for heuristic design rules to parameterize (11) and (12).

2.4 Closed-loop behavior

The transfer function of the controlled system including FF that relates the reference r to the control error e is

$$H(s,\theta) = S(s)(1 - G(s)C_{ff}(s,\theta)). \tag{16}$$

Using Assumption 1 and 2, and implementing (7) in (16) leads to the transfer function approximate

$$H(s,\theta_a,\theta_d) \approx \underbrace{-S(s)\frac{\theta_a}{\hat{m}}}_{H_a(s,\theta_a)} \underbrace{-S(s)\frac{\theta_d s^2}{\hat{m}}}_{H_d(s,\theta_d)}, \tag{17}$$

which describes the contribution of the scalar FF controller parameters θ_a and θ_d in the servo error signal e as function of the set-point r accurately in the frequency range up to the first resonance frequency of the plant.

2.5 Trajectory planning

Motion systems require the movement of one position to another. Point-to-point TP entails the calculation of an allowable time-optimized trajectory $r \in \mathbb{R}$ connecting the current position to a desired future position while avoiding the excitation of the resonance dynamics of the plant and accounting for force and power limitations of the actuators.

Lemma 3. If the set-point trajectory for a motion system described by (1) is restricted to point-to-point moves with the same velocity at the begin and end of the trajectory and with bounds on the first four time-derivatives of position, then the time-optimal trajectory is symmetric and can be calibrated such that the frequency content of the set-point is small compared to the first resonance frequency of the plant.

Proof. Time-optimal trajectories with bounds on the first four time-derivatives of position are obtained by calculating the switching times of the piece-wise constant snap values. The time intervals for a trajectory are completely described by four time intervals: $t_{\bar{d}}$, $t_{\bar{j}}$, $t_{\bar{a}}$, $t_{\bar{v}}$, the constant snap, jerk, acceleration and velocity interval, respectively, see Lambrechts et al. (2005):

$$t_{\bar{d}} = \frac{\bar{j}}{\bar{d}}, \tag{18}$$

$$t_{\bar{j}} = \frac{\bar{a}}{\bar{j}} - t_{\bar{d}}, \tag{19}$$

$$t_{\bar{a}} = \frac{\bar{v} - 2\bar{d}t_{\bar{d}}^3 - 3\bar{d}t_{\bar{d}}^2 t_{\bar{j}} - \bar{d}t_{\bar{d}}t_{\bar{j}}^2}{\bar{d}t_{\bar{d}}^2 + \bar{d}t_{\bar{d}}t_{\bar{j}}}. \tag{20}$$

Here, the constant parameters $\bar{v}$, $\bar{a}$, $\bar{j}$ and $\bar{d}$ are bounds on the velocity, acceleration, jerk and snap, respectively. Hence, the distance covered without the constant velocity phase is fixed:

$$\begin{aligned} x_a = {} & 8\bar{d}t_{\bar{d}}^4 + 16\bar{d}t_{\bar{d}}^3 t_{\bar{j}} + 10\bar{d}t_{\bar{d}}^2 t_{\bar{j}}^2 + 2\bar{d}t_{\bar{d}}t_{\bar{j}}^3 + \bar{d}t_{\bar{d}}^2 t_{\bar{a}}^2 \\ & + \bar{d}t_{\bar{d}}t_{\bar{j}}t_{\bar{a}}^2 + 6\bar{d}t_{\bar{d}}^3 t_{\bar{a}} + 9\bar{d}t_{\bar{d}}^2 t_{\bar{j}}t_{\bar{a}} + 3\bar{d}t_{\bar{d}}t_{\bar{j}}^2 t_{\bar{a}}, \end{aligned} \tag{21}$$

and the constant velocity time interval is given by

$$t_{\bar{v}}(\bar{x}) = \frac{\bar{x} - x_a}{\bar{v}}. \tag{22}$$

So, the reference trajectory is fully characterized as a function of travel distance only. The frequency content of the set-point trajectory r can be expressed as the convolution of unit impulse function ζ with a concatenation of low-pass filters in which the cut-off frequencies are directly related to the time intervals (19)-(20) and (22), i.e., $\omega_{\bar{v}} = \frac{2\pi}{t_{\bar{v}}}$, $\omega_{\bar{a}} = \frac{2\pi}{t_{\bar{a}}}$, $\omega_{\bar{j}} = \frac{2\pi}{t_{\bar{j}}}$, and $\omega_{\bar{d}} = \frac{2\pi}{t_{\bar{d}}}$, see Biagiotti and Melchiorri (2012). The frequency response of the filter composing the TP is given by

$$Q(s,\bar{x}) = \frac{\bar{x}}{s}\left(\frac{1}{t_{\bar{v}}(\bar{x})}\frac{1-e^{-st_{\bar{v}}(\bar{x})}}{s}\right)\left(\frac{1}{t_{\bar{a}}}\frac{1-e^{-st_{\bar{a}}}}{s}\right)\cdot \left(\frac{1}{t_{\bar{j}}}\frac{1-e^{-st_{\bar{j}}}}{s}\right)\left(\frac{1}{t_{\bar{d}}}\frac{1-e^{-st_{\bar{d}}}}{s}\right). \quad (23)$$

The parameters $\bar{v}$, $\bar{a}$, $\bar{j}$ and $\bar{d}$ can be calibrated such that the cut-off frequency of (23) is small with respect to the resonance frequencies in (2). □

Commonly, the velocity $\bar{v}$ and acceleration $\bar{a}$ bounds are directly linked to physical limitations of the actuators while the bounds on jerk and snap can be tuned to reduce excitation of flexible modes of the mechanical structure (Biagiotti and Melchiorri, 2012). Note that, time optimality of the trajectory is only guaranteed for point-to-point moves with active bounds on the first four time-derivatives of position. Hence, it is found that, a time-optimized trajectory for the rest-to-rest case with bounds on the first four derivatives of position can avoid the excitation of the resonance dynamics of the plant and account for force and power limitations of the actuators (Lambrechts et al., 2005; Biagiotti and Melchiorri, 2019).

3. PARAMETER LEARNING FRAMEWORK

This section contains the main result which is the learning framework that provides online adaptation of the FF parameters, to correct for position dependency and time-varying plant behavior.

Note that the parameter learning problem is more involved than the parameter estimation problem: Rather than having the objective to estimate the model parameters that explain the system behavior the aim is to estimate *and* adjust parameters in the system leading to control error improvements in future times.

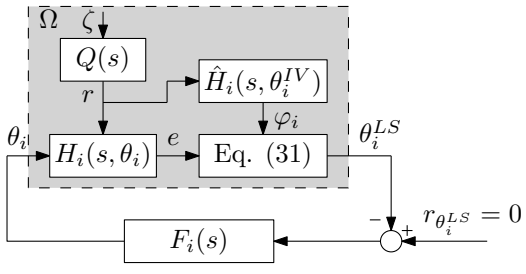

Fig. 2. System representation of the learning feedback interconnection with parameter estimation Ω and parameter adaptation by F_i.

The adaptation of parameters affects, however, the estimation of parameters in future times. Hence, a dependency is obtained in the form of a FB interconnection between, on one hand, the parameter estimation that involves the true FB controlled system, the set-point trajectory as external input, and a parameter estimation algorithm, and, on the other hand, the parameter adaptation, see Fig. 2 for a schematic overview of the FB interconnection.

Here, a learning framework is described that exploits time-scale separation to deal with this dependency by using a two-step recursive approach of relatively fast parameter estimation followed by relatively slow parameter adaptation.

A problem statement is formulated in Section 3.1. The parameter estimation algorithm is further discussed in Section 3.2 and the parameter adaptation in Section 3.3. Moreover, a sketch of the stability analysis of the FB interconnection is provided in Section 3.4.

3.1 Problem description

Offline calibration of θ provides limited accuracy. The required adaptation with respect to the offline calibrated FF parameters is estimated by evaluating the control error $e(t)$ in past times on contributions from sub-optimal FF parameter settings. The learning control objective is to minimize the servo error between the reference signal and the system output by approximating the solution

$$\theta^\star(t) = \arg\min_{\theta(t)} \int_{-\infty}^{t} e^2(\tau,\theta(\tau))\mathrm{d}\tau, \quad (24)$$

in (7), where $\theta^\star(.)$ is the optimal FF parameter signal.

To limit the solution space, a constant parameter estimate is considered in a receding horizon of past measurement data. In this context, we can construct the parameter estimation problem with solution:

$$\theta^\star|_T = \arg\min_{\theta} \int_{t-T}^{t} e^2(\tau,\theta)\mathrm{d}\tau, \quad (25)$$

in which, $\theta^\star|_T$ is a vector of constant parameters for (6) that provides the best fit in the considered horizon of past data. The length of the horizon T gives rise to a trade-off: A short horizon enables a fast adaptation of θ, however, also leads to a larger variation in the parameter estimate.

3.2 Parameter estimation

The parameter estimation problem is thus to find a prediction of the tracking error e (the dependent variable) as defined in (17) given information about the set-point trajectory r (the regressor).

The basis function parameterization of the FF controller (8) in combination with a set-point defined in Lemma 3 allows to consider a scalar prediction error for each FF parameter separately:

$$\epsilon_a(t,\theta_a^\delta) = e(t,\theta) - \tilde{e}_a(\varphi_a(t),\theta_a^\delta), \quad (26)$$

$$\epsilon_d(t,\theta_d^\delta) = e(t,\theta) - \tilde{e}_d(\varphi_d(t),\theta_d^\delta), \quad (27)$$

in which, the tracking error e is possibly corrupted with measurement noise while $\tilde{e}_a$ and $\tilde{e}_d$ are a function of the regressors $\varphi_a(t)$ and $\varphi_d(t)$ and depend on the parameter offsets θ_a^δ and θ_d^δ, respectively. To keep the notation short, in the remainder of the paper the subscript i is used to indicate both the acceleration a and snap d subscripts.

Remark 4. Point-to-point moves defined in Lemma 3 with the begin and end velocity the same results in $\int_{t-T_m}^{t} a(\tau)\mathrm{d}\tau = \int_{t-T_m}^{t} j(\tau)\mathrm{d}\tau = \int_{t-T_m}^{t} d(\tau)\mathrm{d}\tau = 0$, where T_m is the time span of the move. Hence, cross correlation of error e_a by θ_d and vice versa is avoided when considered over one or multiple moves.

To avoid bias in the parameter estimates due to measurement noise, it is required that the prediction error ϵ_i is independent of a particular set of past data (Ljung, 1987; Boeren et al., 2015, 2017). This can be achieved by the application of an additional correlation signal, which is also called IV. The IV signal should be designed in a way that it correlates with the regression variable $r(t)$ but is uncorrelated with measurement noise.

Let us now choose to describe the predictor $\tilde{e}_i$ with a linear regression model (Ljung, 1987):

$$\tilde{e}_i(t, \theta_i^\delta) = \varphi_i(t)\theta_i^\delta, \tag{28}$$

in which the regressor $\varphi_i(t)$ is defined as

$$\varphi_i(t) = \hat{H}_i(t, \theta_i^{IV})r(t). \tag{29}$$

Here, $\theta_i^{IV} \in \mathbb{R}$ is a *selected* sub-optimal compensation parameter with property $\theta_i^{IV} > \theta_i^\star$ and regressor signal φ_i is obtained by convolution of set-point r with an estimate $\hat{H}_i$ of system H_i defined in the right hand side in (17). Note that, signal φ_i resembles a tracking error estimate that is typical for the selected sub-optimal parameter θ_i^{IV}.

Assumption 5. There exists a parameter θ_i for which the system $H_i(s, \theta_i)$ in (17) can be approximated by a low-order continuous-time rational form parametric model approximation:

$$\hat{H}_i(s, \theta_i) = \frac{\sum_{r=0}^{n_q} q_r s^r}{\sum_{r=0}^{n_p} p_r s^r}\theta_i, \tag{30}$$

for which $\sup_{\omega\in[0\ \omega_T]} |H_i(j\omega, \theta_i) - \hat{H}_i(j\omega, \theta_i)| < \epsilon_H$. Here, $\epsilon_H > 0$ is a positive constant, ω_T is the frequency up to which accurate system information is available, and $q_r,\ p_r \in \mathbb{R}$.

The purpose of Assumption 5 is to ensure that, on a horizon $T = \frac{1}{\omega_T}$, an accurate estimate of the (scaled) servo error is obtained while the system's fast dynamics can be disregarded.

Remark 6. The dynamics of high-tech motion systems can be accurately described by $\frac{1}{ms^2}$ in the frequency region up to the first resonance while the low-frequent dynamics of the FB controller are known and described by (11). Furthermore, the bandwidth of the FB is typically also limited by the resonance frequencies of the plant. So, for high-tech motion systems, it is relatively easy to obtain an accurate estimate of the controlled system at least up to the frequency for which rigid-body dynamics hold. The required receding horizon length T is thus directly related to the properties of the mechanical structure. Accurate estimates of the controlled system in the resonant frequency range is more involved however provides opportunities to further shorten the receding horizon length to enable faster parameter estimation.

The size of the prediction error ϵ_i can be measured using a quadratic norm over the horizon of past data, providing a least-squares problem with objective function:

$$V_i(t, \theta_i^\delta) = \frac{1}{T}\int_{t-T}^{t} \left(e(\tau, \theta) - \varphi_i(\tau, \theta_i^{IV})\theta_i^\delta\right)^2 \mathrm{d}\tau. \tag{31}$$

Since (31) is quadratic in the parameter θ_i^δ, setting the derivative of V_i with respect to θ_i^δ equal to zero provides a sufficient condition for optimality leading to parameter estimate:

$$\theta_i^{LS}(t) = \frac{1}{\int_{t-T}^{t} \varphi_i^2(\tau)\mathrm{d}\tau}\int_{t-T}^{t} \varphi_i(\tau)e(\tau, \theta)\mathrm{d}\tau. \tag{32}$$

Note that, the parameter estimate θ_i^{LS} depends on the set-point trajectory excitation within the moving average window and therefore can be time-varying.

3.3 Parameter adaptation

Objective for the learning framework is to adapt the FF parameters given the parameter estimate θ_i^{LS} to improve the servo performance in future time. Due to the dependency of the recursive parameter estimation with the parameter adaptation, immediate application of θ_i^{LS} is not possible as it affects the parameter estimation in future time. Therefore, consider a learning framework that includes adaptation of the FF parameter based on a linear dynamic system:

$$\dot{x}_{\theta_i}(t) = A_i x_{\theta_i}(t) - B_i\theta_i^{LS}(t), \tag{33}$$

$$\theta_i(t) = C_i x_{\theta_i}(t) \tag{34}$$

with transfer function

$$F_i(s) = -C_i(sI - A_i)^{-1}B_i, \tag{35}$$

where the input of this system is the parameter estimate θ_i^{LS} and the output is the adapted FF parameter θ_i. Here, $x_{\theta_i} \in \mathbb{R}^{N_\theta}$, and A_i, B_i, and C_i are to be designed state-space matrices of appropriate size.

3.4 Convergence of the learning framework

The parameter estimation (32) and adaptation (33)-(34) describe a FB interconnection, see again Fig. 2. Time-scale separation provides a way to demonstrate stability of this FB interconnection.

Against this backdrop, the learning control framework is calibrated to operate at two time-scales:

- slowest - the parameter adaptation of θ_i,
- fastest - the parameter estimation of θ_i^{LS}.

Next, a sketch of the convergence analysis is given:

(1) it can be demonstrated using singular perturbation theory that, if the time-scale of the moving horizon in (32), and update rate of θ in (33)-(34), are separated, then the parameter estimation reduces to a memory-less nonlinear function,
(2) it can be demonstrated that, if the set-point trajectory r is bounded and is evaluated over a fixed horizon, then the parameter estimation mapping Ω is a memory-less sector bounded nonlinear function,
(3) it can be demonstrated that, by connecting the above steps, the requirements of the application of the circle criterion are met and the above steps can be aggregated in a theorem for recursive online FF parameter updating.

4. CASE STUDY

This section provides a numerical case study that illustrates the learning framework. Figure 3 displays an example with force input u and position output y. The following parameters are used: $m_1 = m_3 = 1\,\text{kg}$ and $m_2 = 2\,\text{kg}$, $k = 4 \cdot 10^7\,\text{N/m}$ and damping $d = 20\,\text{Ns/m}$.

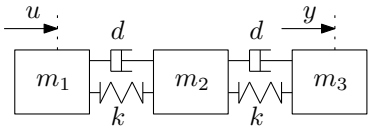

Fig. 3. Three body example.

Furthermore, the idealized PID representation of the FB controller (11) is used, with the following parameterization: $k_d = 1.5708 \cdot 10^3$, $k_p = 5.9218 \cdot 10^5$, $k_i = 3.10 \cdot 10^7$, $\beta_{lp} = 0.5$ and $\omega_{lp} = 250\,\text{Hz}$. Besides two notch filters are tuned with $\beta_p = 0.005$, $\beta_l = 0.1$, $\omega_{nt1} = 1000\,\text{Hz}$ and $\omega_{nt2} = 1420\,\text{Hz}$. Leading to a control bandwidth of ca. 100 Hz. The control system is implemented using a sampling time $T_s = 1 \cdot 10^{-4}\,\text{s}$. The FF control entails acceleration and snap compensation as in (7).

System estimates according to (17) can be generated where, $\theta_a^{IV} = 1.5\hat{m}$, $\theta_d^{IV} = -\hat{m}^2 \frac{1}{\omega_{nt1}^2}$, and the approximate sensitivity function is given by:

$$\hat{S}(s) = \frac{1}{1 + \hat{G}(s)C_{fb}(s)} = \frac{s^5 + 2\beta_{lp}\omega_{lp}s^4 + \omega_{lp}^2 s^3}{s^5 + 2\beta_{lp}\omega_{lp}s^4 + \omega_{lp}^2 s^3 + \frac{k_d\omega_{lp}^2}{\hat{m}}s^2 + \frac{k_p\omega_{lp}^2}{\hat{m}}s + \frac{k_i\omega_{lp}^2}{\hat{m}}}, \quad (36)$$

which includes the known PID and low-pass parameters and the estimated system mass $\hat{m} = 1.02(m_1 + m_2 + m_3)$. The moving average length is based on the control bandwidth, i.e., $T = 0.01\,\text{s}$.

Figure 4 shows the regressor signals during the first move. The learning is applied during consecutive varying moves, see top plane in Fig. 5. The bottom plane of Fig. 5 shows the absolute tracking error. The updated FF parameters are displayed in Fig. 6. It can be seen that the tracking error improves with several orders of magnitude and the FF parameters converge to a value close to the theoretical optimal value. The remaining servo error is due the mismatch of the estimated sensitivity with the true sensitivity function. Further improvement could also be obtained by using six-ed order set-point trajectories in combination with higher-order FF compensation.

5. CONCLUSIONS

This article studied a continuous-time learning framework for online optimization of feedforward (FF) parameters. This framework utilizes a model of the controlled plant in combination with basis functions and selected sub-optimal FF parameters as instrumental variables to recursively estimate the optimal FF parameters. Time-scale separation, between the relatively fast dynamics of parameter estimation in a feedback controlled plant and a relatively slow parameter updating, is exploited to reduce the parameter

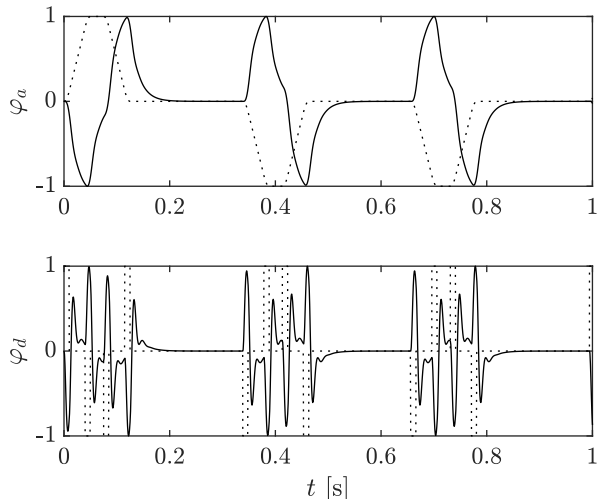

Fig. 4. Normalized acceleration and snap trajectories (dashed, from top to bottom) and normalized regressor signals (solid).

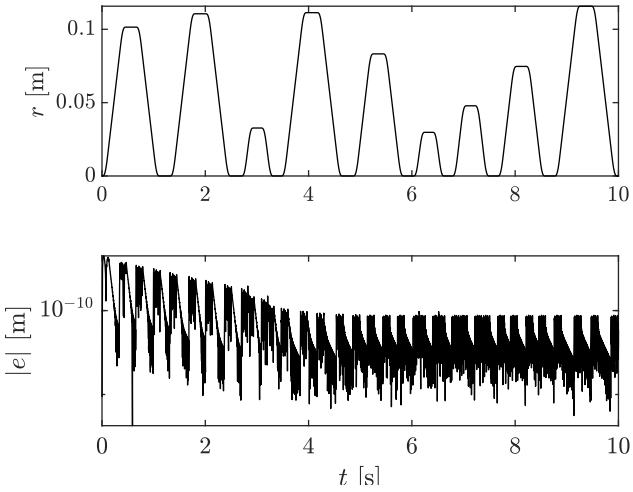

Fig. 5. Set-point trajectory (top) and control error improvement (bottom).

estimation to a memory-less nonlinear function. Furthermore it is sketched that, this nonlinear function is sector bounded. To this end, the circle criterion is applicable to demonstrate convergence with explicit robustness to set-point variations. A numerical case study exemplifies the findings. Future work will focus on providing a rigorous proof for the convergence analysis of the learning framework as well as extending the framework to learning of nonlinear disturbance compensation parameters, e.g., to compensate friction or reluctance disturbance forces.

REFERENCES

Arimoto, S., Kawamura, S., and Miyazaki, F. (1984). Bettering operation of robots by learning. *Journal of robotic systems*, 1, 123–140.

Baggen, M., Heertjes, M., and Kamidi, R. (2008). Data-based feed-forward control in MIMO motion systems. In *American Control Conference*, 3011–3016.

Biagiotti, L. and Melchiorri, C. (2012). FIR filters for online trajectory planning with time- and frequency-

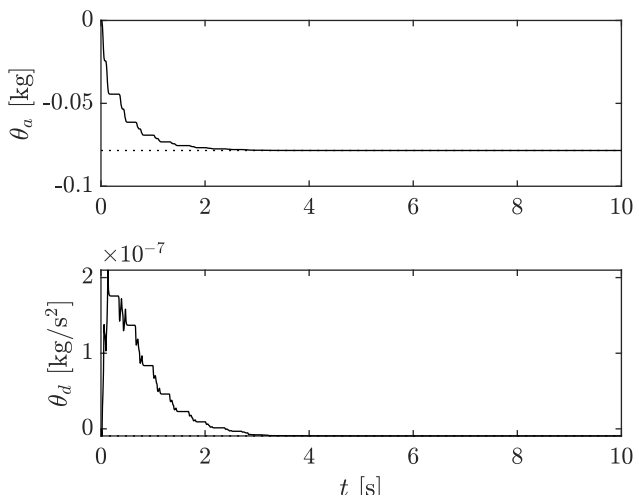

Fig. 6. Evolution of the acceleration and snap feedforward parameters (from top to bottom), the dashed lines indicate the theoretical optimal value.

domain specifications. *Control Engineering Practice*, 20, 1385–1399.

Biagiotti, L. and Melchiorri, C. (2019). Trajectory generation via FIR filters: A procedure for time-optimization under kinematic and frequency constraints. *Control Engineering Practice*, 87, 43–58.

Blanken, L., Koekebakker, S., and Oomen, T. (2020). Data-driven feedforward tuning using non-causal rational basis functions: with application to an industrial flatbed printer. *Mechatronics*, 71.

Boeren, F., Bruijnen, D., and Oomen, T. (2017). Enhanced feedforward controller tuning via instrumental variables: with application to nanopositioning. *International Journal of Control*, 90, 746–764.

Boeren, F., Oomen, T., and Steinbuch, M. (2015). Iterative motion feedforward tuning: A data-driven approach based on instrumental variable identification. *Control Engineering Practice*, 37, 11–19.

Boerlage, M. (2006). MIMO jerk derivative feedforward for motion systems. In *American Control Conference*, 3892–3897.

Boerlage, M., Tousain, R., and Steinbuch, M. (2004). Jerk derivative feedforward control for motion systems. In *American Control Conference*, 4843–4848.

Bolder, J. and Oomen, T. (2015). Rational basis functions in iterative learning control-with experimental verification on a motion system. *IEEE Transactions on Control Systems Technology*, 23, 722–729.

Bristow, D., Tharayil, M., and Alleyne, A. (2006). A survey of iterative learning control: A learning-based method for high-performance tracking control. *IEEE Control Systems Magazine*, 96–114.

Butler, H. (2011). Position control in lithographic equipment: An enabler for current-day chip manufacturing. *IEEE control systems magazine*, 28–47.

Butler, H. (2012). Adaptive feedforward for a wafer stage in a lithography tool. *IEEE Transactions on Control Systems Technology*, 21, 875–881.

Cao, M., Bo, Y., and Gao, H. (2020). Combined feedforward control and disturbance rejection control design for a wafer stage. *Precision Engineering*, 8, 181224–181232.

Heertjes, M., Butler, H., Dirkx, N., van der Meulen, S., Ahlawat, R., O'Brien, K., Simonelli, J., Teng, K.T., and Zhao, Y. (2020). Control of wafer scanners: Methods and developments. In *American Control Conference*, 3686–3703.

Heertjes, M., van de Ven, L., and Kamidi, R. (2017). Acceleration-snap feedforward scheme for a motion system with viscoelastic tuned-mass-damper. In *American Control Conference*, 2888–2893.

Hjalmarsson, H. (2002). Iterative feedback tuning–an overview. *International Journal of Adaptive Control and Signal Processing*, 16, 373–395.

Hoelzle, D., Alleyne, A., and Johnson, A. (2011). Basis task approach to iterative learning control with applications to micro-robotic deposition. *IEEE Transactions on Control Systems Technology*, 19, 1138–1148.

Kara-Mohamed, M., W.P., H., and A., L. (2015). Enhanced tracking for nanopositioning systems using feedforward/feedback multivariable control design. *IEEE Transactions on Control Systems Technology*, 23, 1003–1013.

Krstić, M. and Wang, H.H. (2000). Stability of extremum seeking feedback for general nonlinear dynamic systems. *Automatica*, 36, 595–601.

Lambrechts, P., Boerlage, M., and Steinbuch, M. (2005). Trajectory planning and feedforward design for electromechanical motion systems. *Control Engineering Practice*, 13, 145–157.

Ljung, L. (1987). *System Identification–Theory for the User*. Prentice-Hall.

Mooren, N., Witvoet, G., and Oomen, T. (2019). From batch-to-batch to online learning control: Experimental motion control case study. In *8th IFAC Symposium on Mechatronic Systems and 11th Symposium on Nonlinear Control Systems*.

Mooren, N., Witvoet, G., and Oomen, T. (2022). Online instrumental variable-based feedforward tuning for non-resetting motion tasks. In *preparation*.

Nešić, D., Ying Tan, Manzie, C., Mohammadi, A., and Moase, W. (2012). A unifying framework for analysis and design of extremum seeking controllers. In *2012 24th Chinese Control and Decision Conference (CCDC)*, 4274–4285.

Rotariu, I., Steinbuch, M., and Ellenbroek, R. (2008). Adaptive iterative learning control for high precision motion systems. *IEEE transactions on Control Systems Technology*, 16, 1075–1082.

Söderström, T. and Stoica, P. (1984). *Instrumental Variable Method for System Identification*. Springer-Verlag.

van de Meulen, S., Tousain, R., and Bosgra, O. (2008). Fixed structure feedforward controller design exploiting iterative trials: Application to a wafer stage and a desktop printer. *Journal of Dynamic Systems, Measurement, and Control*, 130.

van de Wijdeven, J. and Bosgra, O. (2010). Using basis functions in iterative learning control: analysis and design theory. *International Journal of Control*, 83, 661–675.

van Zundert, J., Bolder, J., and Oomen, T. (2016). Optimality and flexibility in iterative learning control for varying tasks. *Automatica*, 67, 295–302.